Epoxy coating modification with metal nanoparticles to improve the anticorrosion, migration, and antibacterial properties

Samardžija, Marina; Stojanović, Ivan; Vuković Domanovac, Marija; Alar, Vesna

Source / Izvornik: **Coatings, 2023, 13**

Journal article, Published version
Rad u časopisu, Objavljena verzija rada (izdavačev PDF)

https://doi.org/10.3390/coatings13071201

Permanent link / Trajna poveznica: https://urn.nsk.hr/urn:nbn:hr:169:364988

coatings

MDPI

Article

Epoxy Coating Modification with Metal Nanoparticles to Improve the Anticorrosion, Migration, and Antibacterial Properties

Marina Samardžija [1,*], Ivan Stojanović [2], Marija Vuković Domanovac [3] and Vesna Alar [2]

[1] Department of Chemistry, Faculty of Mining-Geology-Petroleum Engineering, University of Zagreb, 10110 Zagreb, Croatia
[2] Department of Welded Structures, Faculty of Mechanical Engineering and Naval Architecture, University of Zagreb, 10000 Zagreb, Croatia; ivan.stojanovic@fsb.unizg.hr (I.S.); vesna.alar@fsb.unizg.hr (V.A.)
[3] Department of Industrial Ecology, Faculty of Chemical Engineering and Technology, University of Zagreb, 10000 Zagreb, Croatia; mvukovic@fkit.unizg.hr
* Correspondence: marina.samardzija@rgn.unizg.hr; Tel.: +385-1-5535-912

Abstract: Nanoparticles are capable of making more durable and stronger materials with better chemical resistance. They are used for a wide range of applications. Likewise, the potential of metal nanoparticles as antimicrobial agents has been widely studied. In this work, we investigate various nanoparticles (Al, Ni, Ag) incorporated into epoxy coating. The anticorrosion and antibacterial properties of the unmodified and modified coatings were evaluated. According to the SEM and EDS analyses, the coating did not contain agglomerates, which confirms the quality of the dispersion of inorganic nanoparticles in the coating. After 24 h and 10days immersions in a 3.5 wt.% NaCl solution, the corrosion behaviour for all nanocomposite was studied by means of EIS investigations. The study included the evaluation of the inhibition zone of the nanoparticles and the antimicrobial properties of the nanocomposite. It was found that the nanoparticles of Al and Ag provide excellent antibacterial properties. The epoxy nanocomposite with Al NP showed the migration of ions in the range from 0.75 to 1 mg/L in a wastewater solution for 30 days, indicating a potential for antimicrobe activity. The 1% Al NP epoxy nanocomposite showed good anticorrosion and antibacterial properties and demonstrated great potential for applications in pipelines.

Keywords: corrosion protection; nanoparticles; epoxy coating; antibacterial activity

Citation: Samardžija, M.; Stojanović, I.; Vuković Domanovac, M.; Alar, V. Epoxy Coating Modification with Metal Nanoparticles to Improve the Anticorrosion, Migration, and Antibacterial Properties. *Coatings* **2023**, *13*, 1201. https://doi.org/10.3390/coatings13071201

Academic Editor: Jinyang Xu

Received: 9 June 2023
Revised: 1 July 2023
Accepted: 3 July 2023
Published: 4 July 2023

1. Introduction

The 21st century is marked by the study of nanotechnology and the production of nanostructured materials. Nanoparticles (NPs) are a wide class of materials that includes particulate substances with sizes between 1 and 100 nm [1].The use of nanoparticles in different fields such as molecular biology, physics, organic and inorganic chemistry, medicine, and material science is of growing interest in future applications [2]. In recent years, scientists and researchers have been motivated to develop coatings with new features, such as the possibility of the migration of substances due to the improvement of anticorrosive and antibacterial properties. As a result, nanoparticles began to be incorporated into the polymer material. The material obtained was defined as a nanocomposite, which implies a composition of at least two immiscible phases, and one of them in the nanometer scale [3]. The ability of nanocomposite material to release nanoparticles is considered very harmful if applied in the food packaging industry [4], but its application on the surface of drainage pipes is a new idea for protection against microorganisms. Cast iron pipes have been widely used in water distribution systems formore than 150 years due to their high mechanical strength and cost effectiveness [5]. With the development of urbanization and industrialization, the amount of wastewater produced and discharged increased significantly year by year. Consequently, problems such as corrosion, damage, a reduction in the water transport capacity, and an increase in the habitat of pathogenic and opportunistic bacteria

are becoming serious [6,7]. To achieve corrosion protection, organic coatings and corrosion inhibitors are widely used, but the limitations of these materials, such as high cost, heavy contamination, and operational difficulties, has not been completely overcome [8]. Polymer nanocomposite coatings are a new generation of coatings which have recently been used for the protection of drainage pipes from corrosion due to their superior mechanical strength, stiffness, improved barrier properties against oxygen and moisture, increased heat, wear, and use in the simple repair of damaged structures [9,10]. Similarly, a new class of "nanometallo-antibiotics" consisting of numerous metal NPs has appeared, whichinvolves investigating their antimicrobial properties [11]. It is clear that some metal nanoparticles are effective antimicrobial agents against several pathogenic microorganisms, and their action depends on size, shape, and surface charge [12,13]. Mejía and co-authors [14] developed a new thin antibacterial coating with long-term effectiveness based on silver release that has an antibacterial effect. According to the research of Tahir and co-authors, the incorporation of silver nanoparticles (Ag NP) into the epoxy resin reduces the occurrence of bubbling and delamination of the coating and improves the durability of the coating [15]. Epoxy antimicrobial coatings are of great interest for the protection of surfaces, since the survival of microorganisms on the surface environment can be detrimental to materials [16]. Microbially induced corrosion (MIC) can be defined as the process by which biological agents (live organisms) cause changes in the material properties, leading to the structural lowering in quality or value [17]. Considering the proven antibacterial efficacy of metal and metal oxide nanoparticles in an organic coating with clear known mechanisms of action against bacteria for silver, silver oxide, titanium dioxide, iron oxide, and zinc oxide, potential materials with the same effect as nickel and aluminum remain poorly researched [16,18,19].

Nickel is a metal relatively resistant to atmospheric corrosion, but it also has huge potential for the development of antibacterial properties [20,21]. The bactericidal action of nickel nanoparticles (Ni NP) has shown a strong effect with particle sizes in the range of 10–100 nm [21]. Aluminum nanoparticles (Al NP) also have high corrosion resistance, but due to the ability to create a passive oxidation layer their antibacterial potential increases [4]. It can be concluded that certain metal powder nanoparticles have a cytotoxic and genotoxic effect on bacteria, and their intercalation in the epoxy coating creates the potential for antibacterial protection. In this study, the effect of the Al NP, Ni NP, and Ag NP in an epoxy coating on the anticorrosion, migration, and the antibacterial property was investigated. In our current work, the composition and distribution of particles for these coatings were characterized using SEM and EDS investigations. The EIS technique was used to characterize the anticorrosion properties of the modified epoxy coating and epoxy nanocomposite. The migration of nanoparticles from the epoxy coating into the wastewater was observed for 30 d, and the possibility of antibacterial action of nanocomposite was tested according to ISO 22196.

2. Materials and Methods

2.1. Materials

The metallic substrate used during this study was gray cast iron with chemical composition 2.5 C, 1.5 Si, 1.05 Mn, 0.5 P, 0.07 S, and Fe in balance (wt.%). The epoxy coatings that we used in this work were based on diglycidyl ether of bisphenol A, and the polyamine hardener was obtained from Hempel (Umag, Croatia). Aluminum, nickel, and silver nanoparticles with an average particle size of about 100 nm were provided by Guangzhou Hongwu Material Technology Co., Ltd., Guangzhou, China. The morphology of the powder nanoparticles was observed from the SEM micrographs, EDS, and XRF (Figure 1).

According to Figure 1a–c, the Al and Ni NPs showed spherical particles and the Ag NPs within irregular shapes. All nanoparticles showed different sizes. The small nanoparticles had a very large surface area to volume ratio, which gave them huge energy and high reactivity. The agglomerates with average particle sizes from 223.4 to 620.7 nm were observed in Figure 1a,b. The XRF analysis of the elemental composition of the nanoparticle powder showed a high proportion of Al, Ag, and Ni nanoparticles (Table 1).

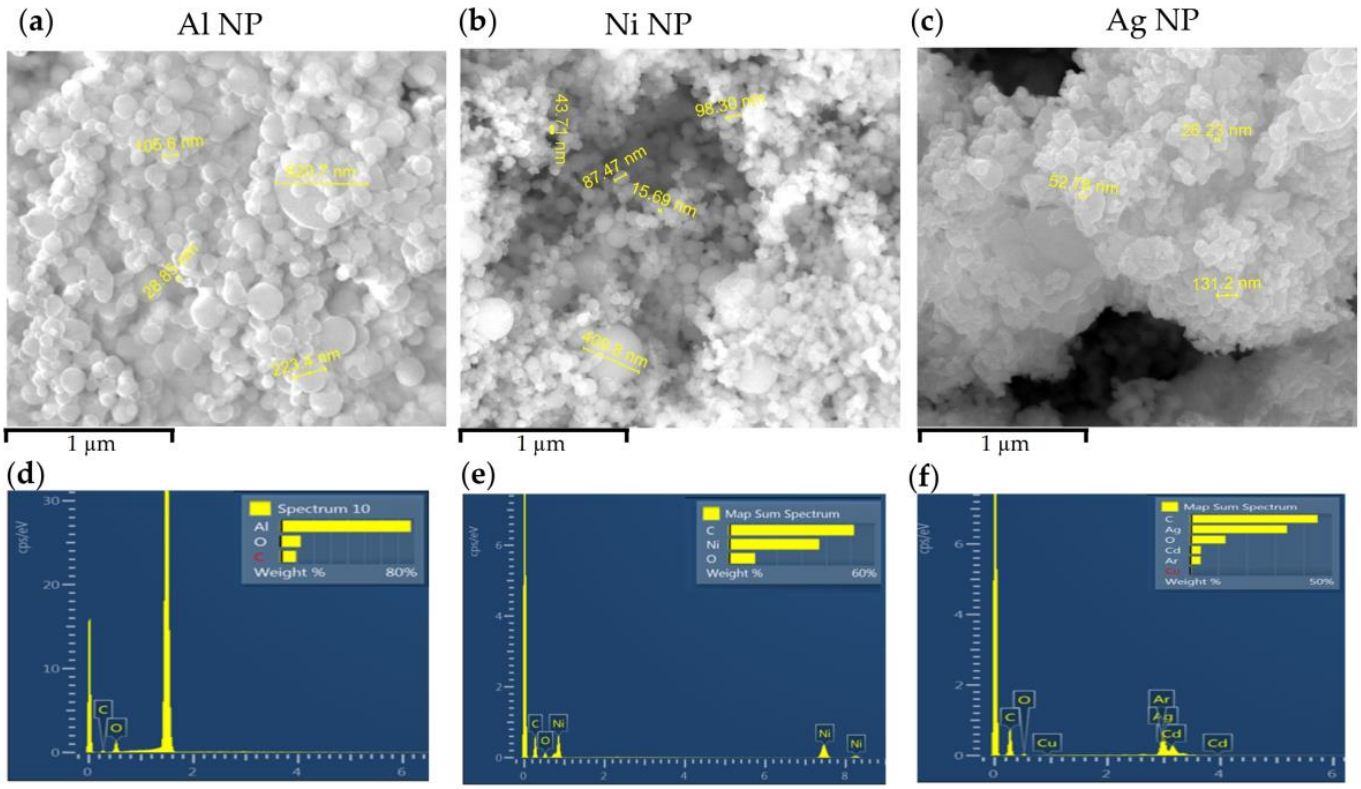

Figure 1. SEM image and EDS analysis of the (**a**,**d**) Al, (**b**,**e**) Ni, and (**c**,**f**) Ag nanoparticles.

Table 1. The XRF analysis of the elemental composition of the nanoparticle powder.

Al NP			Ni NP			Ag NP		
Elements	**wt.%**	**+/−**	**Elements**	**wt.%**	**+/−**	**Elements**	**wt.%**	**+/−**
Al	98.85	0.24	Ni	99.21	0.25	Ag	98.94	0.32
Cr	0.08	0.01	Cu	0.28	0.05	Cr	0.41	0.10
Fe	0.03	0.43	Si	0.26	0.05	Co	0.33	0.04
Residue	1.04	0.01	Co	0.11	0.02	Si	0.33	0.02
Total	100	-	Residue	0.14	0.01	Total	100	-
			Total	100				

2.2. Preparation of the Epoxy Coating/Nanocomposite

The epoxy coating was formulated by taking epoxy paint and polyamine hardener in the mass ratio of 4:1. Four formulations of prepared coatings are shown in Table 2.

At ambient temperature, various nanoparticles were incorporated into the epoxy coating under sonicate agitation for 20 min with a delay in the process due to the cooling of the nanocomposite. Polyamine hardener was added to the nanocomposite and mechanically stirred using a glass stirrer.

Before applying the coating, the panels of 9.5 cm × 0.9 cm × 15 cm gray cast iron were abrasively blasted and cleaned with ethanol (70 wt.%). The nanocomposite mixture was applied using a film applicator with a wet film thickness of 150 µm. The samples were kept at room temperature for 24 h, and then another layer of nanocomposites was applied in the opposite direction. The samples were left at room temperature (25 °C) for 7 days.

Table 2. The chemical composition of the tested samples.

Sample	Epoxy Coating (g)	Hardener (g)	m (Al NP) (g)	m (Ni NP) (g)	m (Ag NP) (g)	Thickness (µm)
Epoxy Coating	30	7.5	-	-	-	249.1
1% Al NP Nanocomposite	30	7.5	0.4545	-	-	256.1
1% Ni NP Nanocomposite	30	7.5	-	0.4545	-	266.5
1% Ag NP Nanocomposite	30	7.5	-	-	0.4545	264.9

2.3. Characterization of the Epoxy Coating/Nanocomposite

To evaluate the size of the nanoparticles, the quality of dispersion, and the appearance of the agglomerate of nanoparticles in the nanocomposite, scanning electron microscopy (SEM) (TESCAN Brno, Brno, Czech Republic) and energy-dispersive X-ray spectroscopy (EDS) analyses were used.

To investigate the anticorrosion behavior of Al, Ni, and Ag nanocomposites, electrochemical impedance spectroscopy (EIS) (VersaSTAT 3, AMETEK Scientific 131 Instruments, Princeton applied research, Berwyn, PA, USA) was used. These measurements were performed in a three-electrode electrochemical cell in a 3.5 wt.% NaCl solution. The coated gray cast iron was used as the working electrode, with a test area of 19.75 cm^2, a saturated calomel electrode was used as a reference electrode, and the graphite electrode was used as an auxiliary electrode. The frequency scan range of 0.1 to 10^5 Hz with an amplitude of 10 mV was used. The impedance data were fitted using the ZSimpWin software(AMETEK, Berwyn, PA, USA) (Version 3.2).

The samples of epoxy coating, 1% Al NP epoxy nanocomposite,1% Ni NP epoxy nanocomposite, and 1% Ag NP epoxy nanocomposite were placed in contact with simulation wastewater according to the DIN EN 877 [22]. For the assessment of Al^{3+}, Ni^{2+}, and Ag^{+} ions' migration from the epoxy coating, 10 g of each sample was immersed in 100 mL simulated wastewater for 30 days. In this study, samples were kept in the dark at a temperature of 40 °C. The temperature for this study was chosen according to the real conditions in drainage pipes. The mass concentration, electrical conductivity, and pH value of the wastewater were determined after 10, 20, and 30 days.The mass concentration of Al^{3+}, Ni^{+}, and Ag^{+} ions in wastewater was determined with the flame atomic absorption spectrometry (F-AAS) technique (Perkin Elmer Analyst 700, Waltham, MA, USA).The conductivity and pH values were measured with a pH/EC meter (HI5521–02, HANNA instruments, Woonsocket, RI, USA).

The antibacterial properties of the Al, Ni, and Ag were investigated with a well-diffusion method [23]. For this purpose, *P. aeruginosa* was used as a Gram-negative bacterial strain, and *B. subtills* as a Gram-positive bacterial strain. The 24 h aged active bacterial cultures were poured into the Muller Hinton culture medium. The nanoparticle samples dissolved in distilled water (100 g/mL) were added from the stock into each well. The zone of inhibition was measured using a ruler. After 24 h, the appearance of the inhibition zone was observed.

The antibacterial activities of nanocomposites were tested according to ISO 22196:2011 against *P. aeruginosa* and *B. subtilis* [24]. The surface of the epoxy coating, 1% Al epoxy nanocomposite, 1% Ni epoxy nanocomposite, and 1% Ag epoxy nanocomposite were cut to size 50 mm × 50 mm and inoculated with 0.4 mL of 10^5 CFU bacterial suspensions. All samples were covered with polyethylene foil dimensions of 40 mm × 40 mm (± 1 mm) and a thickness of 0.06 mm. All samples were placed in a Petri dish and incubated at 35 °C (±1 °C) and 90% relative humidity (RH) (±5%) for 24 h (±1 h). The number of viable bacterial cells was determined by plating different dilutions on plate count agar, incubating the plates for 24 h at 37 °C, and then visually counting the colonies [25]. All experiments are representative of repeated trials. Sample error bars on plots represent ± SD. The

measurement of the inhibition zone was carried out in four sections (rotation by 45°) using a ruler with a length of 15 cm. The measurements were repeated three times.

3. Results and Discussion

3.1. SEM and EDS Analysis of Epoxy Coating/Nanocomposite

The morphology of epoxy coating and 1 wt.% of Al, Ni, and Ag nanocomposites were investigated using SEM analysis. Figure 2a shows the SEM images of epoxy coating without nanoparticles, which indicates a rough surface morphology with a large addition of other coating components such as fillers, additives, pigments and similar. The EDS analysis confirms the presence of aluminum particles in the initial sample (Figure 2b,c). It was assumed that these microparticles of aluminum were used as a pigment in the epoxy coating. The presence of these particles in the initial epoxy coating showed small irregularities and the appearance of agglomerates (Figure 2b). The EDS analysis of the initial epoxy coating (Figure 2c) determined the percentage of the aluminum microparticles, and this was 0.85%.

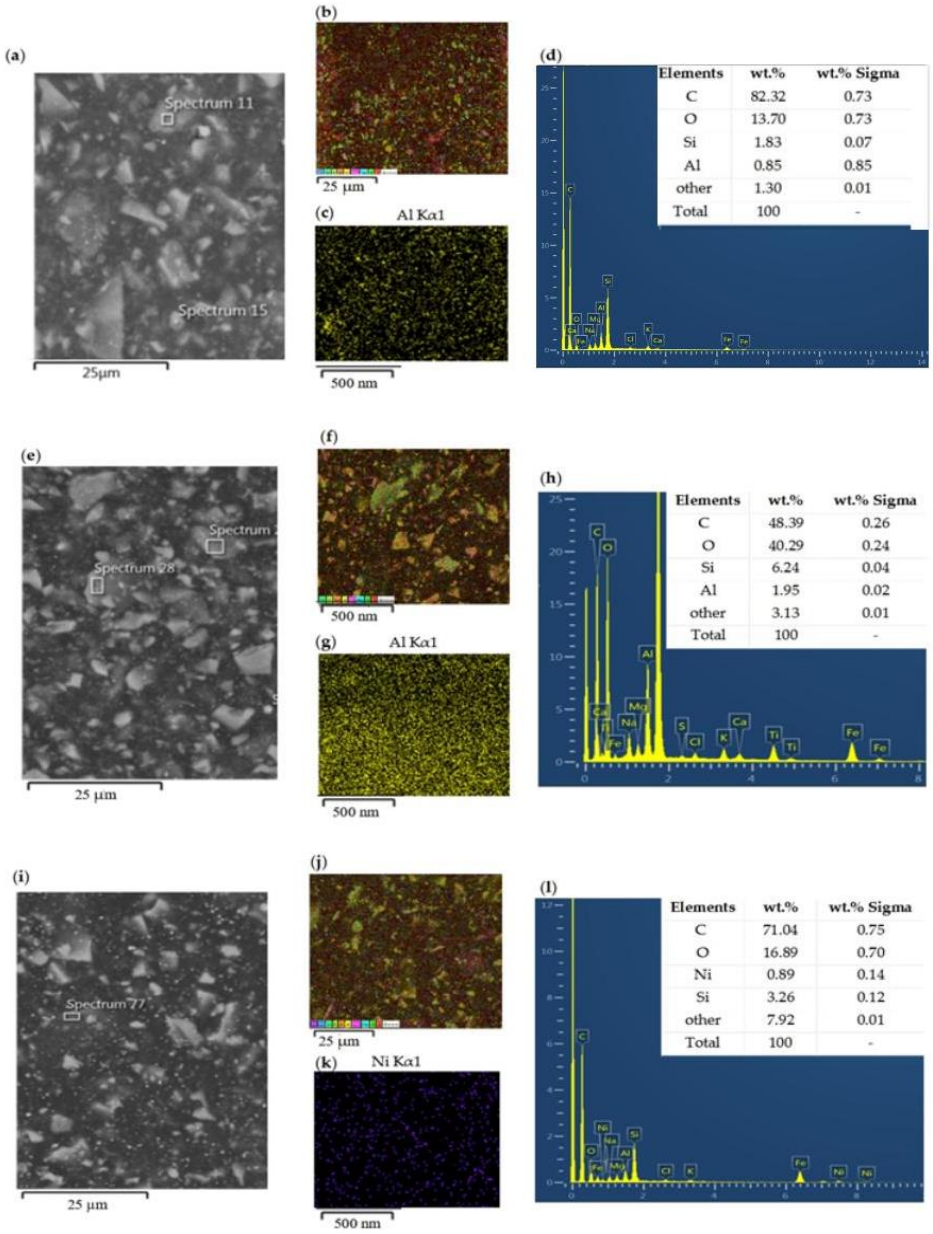

Figure 2. *Cont.*

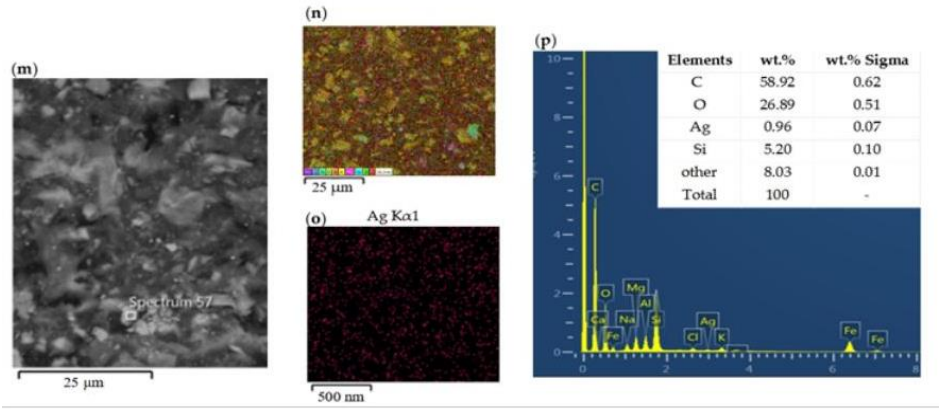

Figure 2. The SEM and EDS analyses of (**a**,**b**) epoxy coating, (**e**,**f**) 1% Al NP epoxy nanocomposite, (**i**,**j**) 1% Ni NP epoxy nanocomposite, and (**m**,**n**) 1% Ag NP epoxy nanocomposite. The EDS mapping and element weight percentages of distribution of microparticles of (**c**,**d**) Al in epoxy coating, and nanoparticles of (**g**,**h**) Al, (**k**,**l**) Ni, and (**o**,**p**) Ag in the nanocomposite.

With the addition of nanoparticles, the rough surface morphology of nanocomposites remained the same (Figure 2e,i,m).The action of the sonication process improved the distribution of the added aluminum particles (Figure 2g). The EDS analysis confirmed the uniform distribution of Ni and Ag nanoparticles within the epoxy coating, shown in Figure 2k,o. Furthermore, EDS analysis determined that all nanocomposite samples contained a certain percentage of nanoparticles that deviated very slightly from the added 1% nanoparticles (Figure 2d,h,l,p).

3.2. EIS Analysis of Epoxy Coating/Nanocomposite

The EIS measurements were performed to investigate the effects of the addition of Al, Ni, and Ag nanoparticles on the corrosion protection properties of the epoxy coating in a 3.5 wt.% NaCl solution with different immersion times. According to the electrochemical behavior of the various prepared nanocomposites, the model of the equivalent circuit with three resistance elements was chosen (Figure 3). This model demonstrated electrolyte resistance, R_e, coating capacitance, CPE_{coat}, coating resistance, R_{coat}, charge transfer resistance, R_{ct}, and double layer capacitance, CPE_{dl} [26]. The behavior of the CPE was shown by the parameter phase shift, n ($-1 \leq n \leq 1$); when $n = 0$, the CPE represented a pure resistor, if $n = -1$, the CPE stood for an inductor, and if $n = +1$, the CPE represented a pure capacitor [27].

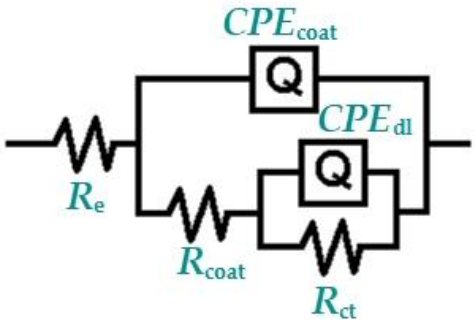

Figure 3. The equivalent circuits used for fitting the Nyquist and Bode plots for coating.

The Nyquist and Bode plots for the epoxy coating, 1% Al epoxy nanocomposite, 1% Ni epoxy nanocomposite, and 1% Ag epoxy nanocomposite after 24 h and 10 days of immersion in 3.5 wt.% NaCl solution are illustrated in Figure 4a–d. The calculated values

of the EIS parameters were reported in Table 3. The coating protection efficiency (%*CPE*) also listed in the table was calculated using the equation [28]:

$$\%CPE = \frac{R_{\text{coat with NP}} - R_{\text{coat without NP}}}{R_{\text{coat with NP}}} \quad (1)$$

where $R_{\text{coat with NP}}$ is the resistance of Al, Ni, or Ag nanocomposites, and $R_{\text{coat without NP}}$ is the resistance of the epoxy coating.

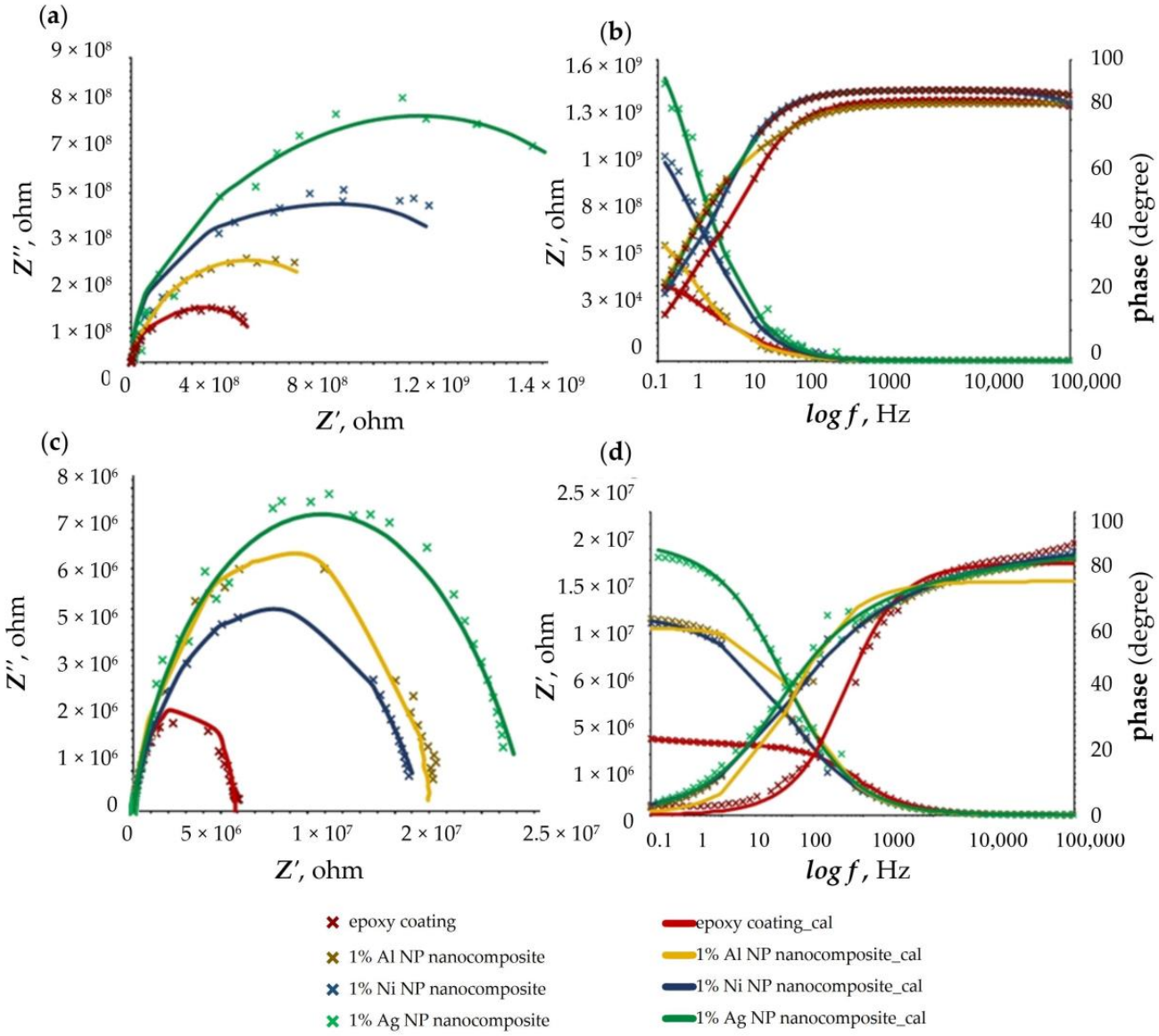

Figure 4. The (**a**,**c**) Nyquist and (**b**,**d**) Bode plots for epoxy coating, 1% Al epoxy nanocomposite, 1% Ni epoxy nanocomposite, and 1% Ag epoxy nanocomposite after (**a**,**b**) 24 h and (**c**,**d**) 10 days of exposure to 3.5 wt.% NaCl solution.

After immersion, as shown in Figure 4, the electrochemical response of the prepared nanocomposites showed one-time constants. The Nyquist diagrams for epoxy coating had the lowest value of R_{coat}, implying that the presence of nanoparticles prolonged the use of the gray cast iron. The nanocomposite with 1% of Ag NP showed the best corrosion resistance, followed by the 1% Ni NP nanocomposite and 1% Al NP nanocomposite (Figure 4a). All samples achieved a constant phase angle value extending from the medium frequency range (100 Hz) to the high frequency range (10^5 Hz) after 24 h exposure in

3.5 wt.% NaCl solution (Figure 4b). With increasing immersion time (after 10 days), the resistance decreased due to the penetration of the electrolyte through the nanocomposite layer, and the corrosion resistance for 1% Ni and 1% Al nanocomposites became equal (Figure 4a,c). Figure 4c shows the deviation of the Nyquist diagrams from a perfect semicircle. This phenomenon is referred to as frequency dispersion, and has been attributed to the roughness and non-uniformity of a working electrode, fracture structures, and the formation of porous layers [29]. This behavior can be observed in the Bode diagram, where the constant area of the phase angle value decreased, indicating that all samples had started to degrade (Figure 4d).

Table 3. Electrochemical parameters of the EIS experiments for all sample after 24 h, and 10 days of exposure to 3.5 wt.% NaCl solution at room temperature.

Samples	R_e, Ω	R_{coat}, Ω	CPE_{coat}, Ssec^n	n	R_{ct},Ω	CPE_{dl}, Ssec^n	n	CPE, %
After 24 h								
Epoxy Coating	195.9	2.55×10^8	4.8×10^{-10}	0.9641	1.76×10^8	2.32×10^{-9}	0.9305	-
1% Al NP Nanocomposite	116.8	5.68×10^8	6.97×10^{-11}	0.9379	2.034×10^8	5.67×10^{-10}	0.9505	54.87
1% Ni NP Nanocomposite	204.1	7.90×10^8	2.72×10^{-12}	1	4.42×10^8	1.69×10^{-9}	1	67.72
1% AgNP Nanocomposite	217.1	8.89×10^8	5.95×10^{-12}	1	8.81×10^8	2.12×10^{-10}	1	71.32
After 10 days								
Epoxy Coating	153.9	5.87×10^6	7.35×10^{-10}	0.924	4.87×10^4	4.19×10^{-9}	0.9951	-
1% Al NP Nanocomposite	100.0	1.67×10^7	5.63×10^{-10}	0.9102	2.35×10^6	3.85×10^{-10}	0.9862	64.85
1% Ni NP Nanocomposite	165.3	2.34×10^7	1.32×10^{-11}	0.9589	3.34×10^6	7.53×10^{-10}	0.9357	74.91
1% AgNP Nanocomposite	135.5	2.57×10^7	3.64×10^{-11}	0.9525	4.73×10^6	9.23×10^{-10}	0.9768	77.16

Based on Table 3, the double layer capacitance between the coating surface/electrolyte solutions (CPE_{coat} value) increased with time. This showed that the absorption level of the electrolyte solution in the nanocomposite had increased, but its resistance was still better than that of the epoxy coating. Further inspection of the table revealed that the n values were close to unity, implying that the interface behaved nearly capacitively. The addition of nanoparticles increased the value of %CPE. In all nanocomposites, the efficiency improved with time. The reason for such behavior could be nanoscale inorganic particles that cause better barrier properties. When metals interact with their surroundings, they can be converted into a more chemically stable form such as oxide, hydroxide, or sulfide, and thus provide better corrosion resistance [30,31].

Figure 5 illustrates the reaction between Al, Ni, and Ag NP and electrolyte, and the protection mechanism of the Al, Ni, and Ag nanocomposites in contact with corrosive electrolyte. When metallic aluminum comes into contact with oxygen, it becomes very reactive. A thin layer of alumina (4 nm thickness) forms in about 100 picoseconds on any exposed aluminum surface, which acts as a protective covering for further oxidation [32]. The Al NPs form an aluminum oxide layer on its surface in contact with the electrolyte, according to the following equations [33]:

$$2Al + 6H_2O \rightarrow 2Al(OH)_3 + 3H_2 \quad (2)$$

$$2Al + 4H_2O \rightarrow 2AlO(OH) + 3H_2 \quad (3)$$

$$2Al + 3H_2O \rightarrow 2Al_2O_3 + 3H_2 \quad (4)$$

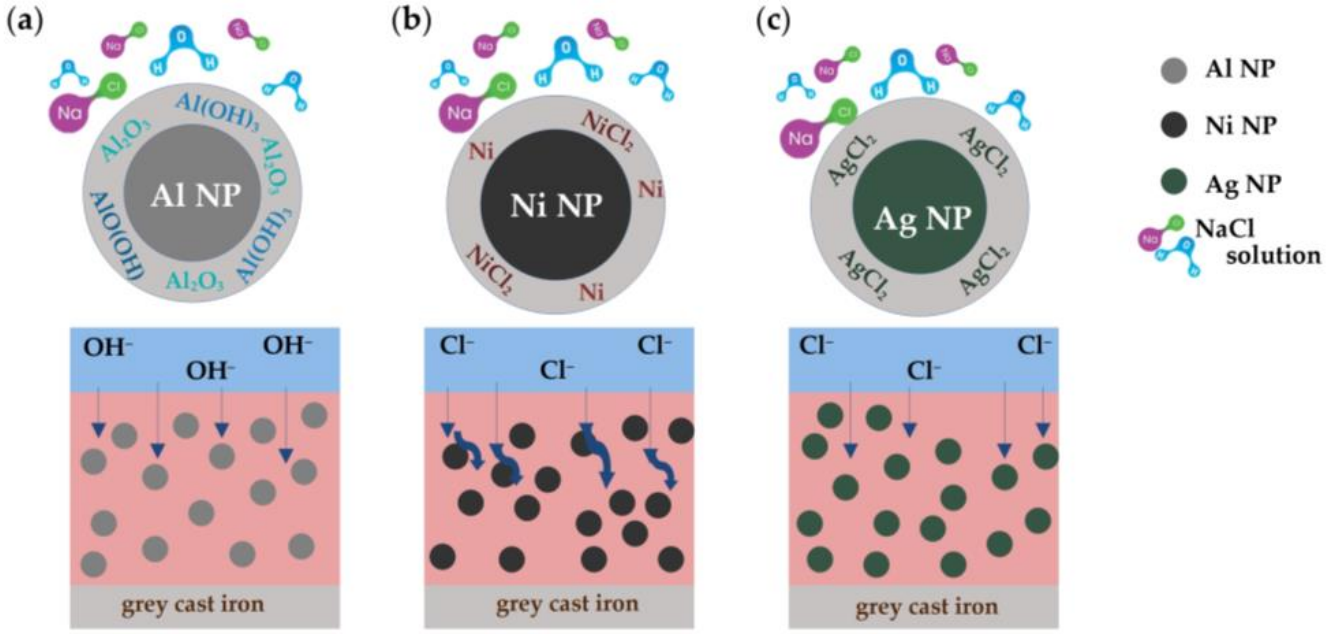

Figure 5. Protection mechanisms of (**a**) Al, (**b**) Ni, and (**c**) Ag nanoparticles in the epoxy coating in contact with NaClsolution.

The volume of formed aluminum oxides is greater than the volume of nanoparticles, which can prevent the further penetration of the corrosive medium, prolong the path of penetration of the corrosive medium into the coating, and ultimately delay the onset of corrosion (Figure 5a) [34,35].

The Ni NPs did not show passive behavior in the epoxy coating because the 3.5 wt.% NaCl solution had a pH value of7. Nickel did not react with water, and small amounts of chloride ions can be exposed on its surface. According to Pourbex's diagram, passive oxide films should appear at a pHvalue of 10 [20,36]. From these results, we can conclude that only Ni NPs and a small part of the formed $NiCl_2$ acted to increase the corrosion resistance of nickel nanocomposites. The nickel nanocomposite system did not have the ability to close the micropores formed in the epoxy coating during exposure to a corrosive medium. The effectiveness of this coating dropped, as can be seen in Figure 4c,d.

The Ag NPs have the property of releasing Ag^+ ions, which gives them the ability to react with other chemical species in the environment. Since silver is a noble metal ($E^\circ/V = 0.79$ vs. SHE), its affinity for oxygen will be low, so a layer of AgCl will form on its surface when exposed to 3.5 wt.% NaCl solution [36,37]. The generation of insoluble AgCl leads to the formation of a chemical barrier inside the epoxy coating. Ag NPs act as a chemical barrier against the further penetration of corrosive species from the electrolyte to the grey cast iron substrate [38].

3.3. Antibacterial Activity of the Al, Ni, and Ag Nanoparticles

The antibacterial activity of Al, Ni, and Ag nanoparticles was tested against various bacterial strains: *P. aeruginosa*, and *B. subtilise.* Figure 6 represents the antibacterial activity of nanoparticles for various bacteria in a well-diffusion technique. Arithmetic means of measurement results are given with measurement uncertainty U = 1.5 mm, k = 2, and P = 95%, where U is expanded measurement uncertainty, k the presented coverage factor, and P is confidence level.

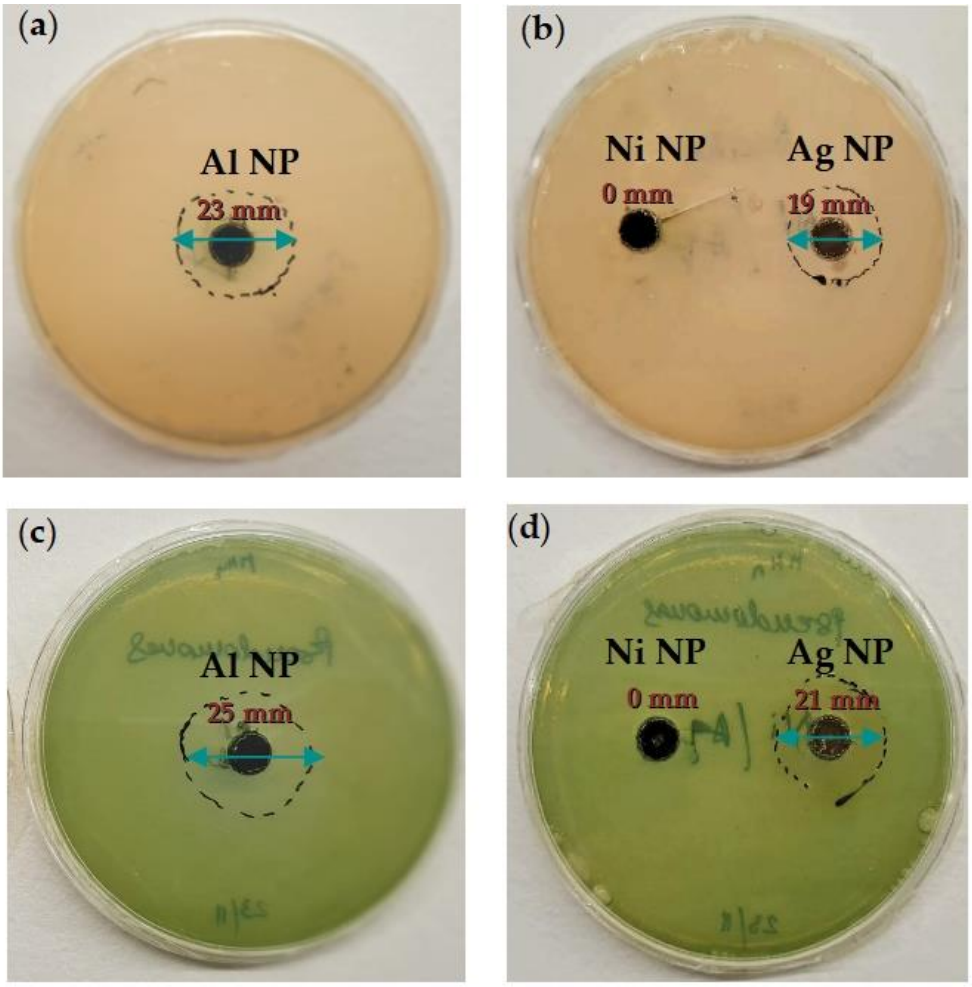

Figure 6. Zone of inhibition of (**a**) Al, and (**b**) Ni, and Ag nanoparticles against *B. subtilis*, and (**c**) Al, and (**d**) Ni, and Ag against *P. aeruginosa*.

The results indicated that Al and Ag nanoparticles showed effective antibacterial activity compared to Ni nanoparticles. The diameter of the inhibitory zone shows that Al NP had a larger zone of inhibition than Ag NP. In this respect, it was found that the Al and Ag NP were poisonous to both Gram-positive and Gram-negative bacteria. Nickel nanoparticles showed a very small inhibition zone, due to the large range of nanoparticle sizes. Typically, smaller NPs have better interaction with the bacteria due to their ability to penetrate a cell and inhibit bacteria growth [11,13]. Asghari and co-authors revealed that *P. aeruginosa* showed a high survival rate against Ni NPs and therefore can survive at quite high concentrations of Ni NPs [39]. It was assumed that due to their large size range and the possibility of agglomeration in aqueous media, Ni NPs could not enter the membrane of bacterial cells (*P. aeruginosa* and *B. subtilis*) to attach to functional groups of proteins to cause their denaturation [40].

3.4. Migration Ability and Antibacterial Activity of the Nanocomposites

A migration of nanoparticles from epoxy coating is a very important test because it provides a new property for drainage pipe protection. Figure 7 demonstrated the migration of Al and Ni nanoparticles from the epoxy coating into simulated wastewater. Released Ag^+ ions from the epoxy coating reacted with Cl^- ions from the wastewater to form a white precipitate of silver(I) chloride. This is the reason why the actual concentration of Ag^+ ions released could not be determined with F-AAS techniques. In Figure 7, the concentration of Ag^+ ions in the wastewater was below the detection limit of the instrument.

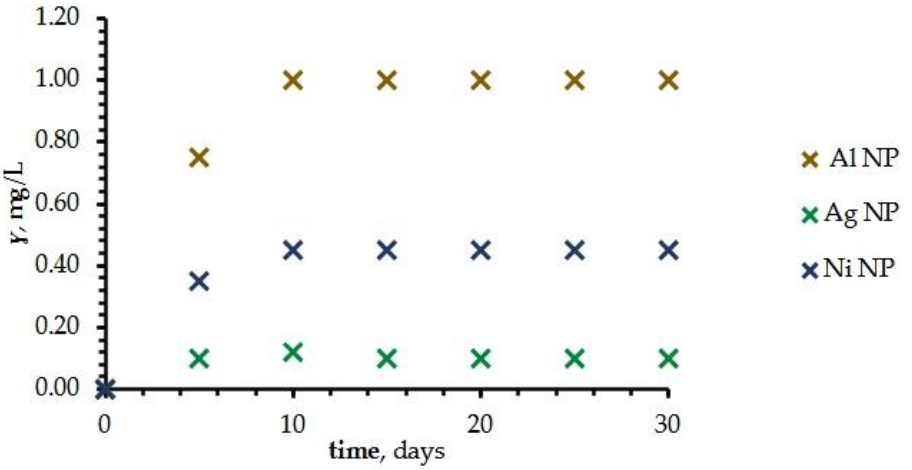

Figure 7. The mass concentration of the migration of Al, Ag, and Ni nanoparticles from epoxy coating to simulated wastewater.

The nanoparticles with 1% of Al NP showed significant migration, while nanocomposites with Ag and Ni nanoparticles showed the lowest value of migration from epoxy coating to the wastewater (Figure 7). The amount of migrated Al NP gradually increased in the beginning, but after 10 days of exposure the wastewater assumed a constant value of aluminum concentration (1 mg/L).For all samples, the pH-value increased very slightly, from 7.723 to 8.791, while the electrical conductivity showed a significant increase for the Al NP nanocomposite, from 1.085 to 2.083 mS/cm.

The migration of nanoparticles from the epoxy coating was stimulated by the action of the wastewater. Aluminum nanoparticles were the only ones capable of forming an oxide film on their surface. The resulting oxide film, with its passivity, closed the micropores of the epoxy and did not allow the oxidation and migration of other nanoparticles located further from the surface of the epoxy coating. The incorporation of certain metals and metal-oxides in the epoxy polymers also led to the development of 'active' materials that prevented the growth of microorganisms, and hence preserved the quality of water pipesduring the transportation of wastewater. According to ISO 22196, the antibacterial properties of the epoxy coating (control sample) and nanocomposites were determined by measuring the reduction in antibacterial activity. Consistent with the ISO guidelines, the reduction in antibacterial activity was estimated using the following equation [41]:

$$\text{reduction of antibacterial activity} = \frac{(CFU_{0h} - CFU_{24h})}{CFU_{0h}} \times 100 \quad (5)$$

where CFU_{0h} is the bacterial colony forming units obtained for the control samples before incubation, and CFU_{24h} is the bacterial colony forming units observed for the test conditions for the nanocomposites after incubation.

The antibacterial activity of the epoxy coating and nanocomposites against *P. aeruginosa* and *B. subtilis* after a 24 h exposition period is presented in Figure 8 and the reduction in antibacterial activity in Table 4.

Table 4. Average values of bacterial reductions of epoxy coating and 1% Al NP, 1% Ag NP, and 1% Ni NP in nanocomposite against *P. aeruginosa* and *B. subtilis* after 24 h.

		Nanocomposite		
	Epoxy Coating	**1% Al NP**	**1% Ag NP**	**1% Ni NP**
P. aerugionosa	4.17 ± 0.09	61.46 ± 2.64	45.83 ± 4.05	11.46 ± 0.92
B. subtilis	3.44 ± 0.11	55.31 ± 0.16	42.19 ± 1.41	11.25 ± 0.15

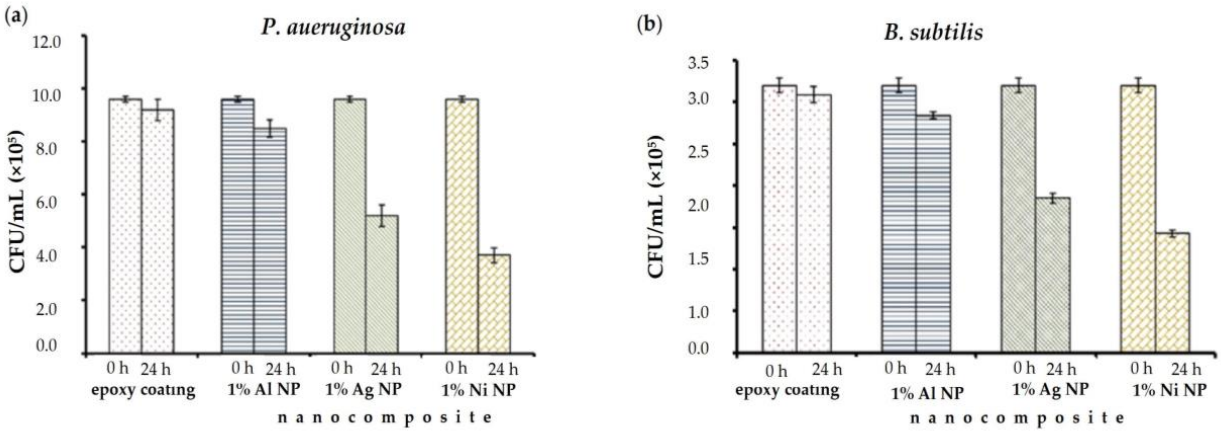

Figure 8. Antibacterial activity of epoxy coating, and 1% Al, 1% Ag, and 1% Ni epoxy nanocomposite on (**a**) *P. aerugionosa* and (**b**) *B. subtilis* during 24 h according to the ISO 22196 standard.

Based on the evaluation of bacteria (Figure 8), we concluded that after 24 h incubation the highest live count of *P. aeruginosa* and *B. subtilis* was observed on the epoxy coating samples and samples containing 1% of Ni NP in the nanocomposite (Table 4). The nanocomposite with 1% of Al NP exhibited the highest antibacterial effect, with a reduction of 61.46 ± 0.09% for *P. aeruginosa* and 55.31 ± 0.16% for *B. subtilis* (Figure 8, Table 4). The 1% of Ag NP in the epoxy coating showed the second-greatest antimicrobial potential, and achieved a 45.83 ± 4.05% cell reduction for *P. aeruginosa* and 42.19 ± 1.41% for *B. subtilis*, respectively, after 24 h incubation. However, the average leaching potential of Al NP was better than Ag NP in the epoxy coating (Figure 7). In contact with aqueous media, the Al NP formed an aluminum oxide and smaller amounts of aluminum hydroxide and oxyhydroxide [34]. The attraction between nanoparticles and bacteria depends on the surface charge of the nanoparticles and the bacteria [42]. Gram-positive bacteria (*B. subtilis*) consist of a thick layer of peptidoglycan, which is embedded in teichoic acid, while Gram-negative bacteria (*P. aeruginosa*) have a layer of lipopolysaccharide at the external surface. The teichoic acid and lipopolysaccharides impart a negative charge to the surface of bacterial cells [43]. The negatively charged bacterial surfaces of *P. aeruginosa* and *B. subtilis* strongly attract the resulting highly positively charged oxides, for example Al_2O_3 [44]. Better electrostatic attraction between bacteria and particles will result in better antibacterial action, which is visible in Figures 6c and 8a. Table 4 shows that less antibacterial activity was evident in samples exposed to the bacterium *B. subtilis* due to the thick outer cell wall, which can hinder NP penetration into the thick peptidoglycan layer.

In contact with corrosive media, Al NPs react with water molecules and the following redox reactions occur [45]:

$$Al(s) + 6H_2O(l) \rightarrow 2Al^{3+}(aq) + 6OH^{-}(aq) + 3H_2(g) \quad (6)$$

In the oxidation reaction, the Al^{3+} ion is formed, which is toxic to bacteria. Also, the resulting oxidation products can release the Al^{3+} ion, which will affect the life of the bacteria [41]. The mechanism of action of Al^{3+} ions has not been fully clarified yet. Cell penetration and the adsorption or diffusion of NPs at the cell surface is often the initial step in the stages involved in some microbial cell inhibition [46]. According to literature [47], an increased Al^{3+} concentration can stimulate reactive oxygen species (ROS), which can act as the main factor in DNA damage in bacterial cells.

4. Conclusions

The influence of nanoparticles in the epoxy coating leads to the modification of the internal defects in the coating due to the filling of voids and blocking of easy access to channels. Nanoparticles that could react with a corrosive medium prolong the path of

penetration of corrosive species from the electrolyte to the metal substrate. Likewise, the resulting corrosion product on the nanoparticle is dangerous for lower organisms and can be used for the formation of a new property of the coating. These studies showed that Al and Ag nanoparticles embedded in nanocomposites can significantly improve the anticorrosive properties and inhibit bacteria, while Ni NPs have lower efficiency. Due to remarkable properties like high reactivity, the ability to form a homogeneous structure, bacterial resistance, cost-effectiveness, and unexplored literature, Al NPs attracted our enormous interest and will continue to serve for detailed analysis so that they can be applied as a protective additive in epoxy coating for the protection of pipelines.

Author Contributions: Conceptualization, M.S., V.A. and M.V.D.; methodology, M.S. and M.V.D.; software, M.S.; validation, M.S. and M.V.D.; formal analysis, M.S.; investigation, M.S. and M.V.D.; resources, V.A. and I.S.; data curation, M.S.; writing—original draft preparation, M.S.; writing—review and editing, M.S.; visualization, M.S.; supervision, V.A., I.S. and M.V.D.; project administration, V.A. and I.S.; funding acquisition, V.A. All authors have read and agreed to the published version of the manuscript.

Funding: This research was funded by "Development of anticorrosion protection system for multipurpose pipe use", Grant Number KK.01.1.1.07.0045. This work was supported by the European Regional Development Fund under the Operational Program Competitiveness and Cohesion 2014–2020.

Institutional Review Board Statement: Not applicable.

Informed Consent Statement: Not applicable.

Data Availability Statement: Not applicable.

Acknowledgments: We thank Michaela Hruškova Hasan (University of Zagreb, Faculty of Mining, Geology, and Petroleum Engineering) for the use of flame atomic absorption spectrometry techniquesand helpful advice.

Conflicts of Interest: The authors declare no conflict of interest.

References

1. Khan, I.; Saeed, K.; Khan, I. Nanoparticles: Properties, applications, and toxicities. *Arab. J. Chem.* **2019**, *12*, 908–931. [CrossRef]
2. Jamkhande, P.G.; Ghule, N.W.; Bamer, A.H.; Kalaskar, M.G. Metal nanoparticles synthesis: An overview on methods of preparation, advantages and disadvantages, and applications. *J. Drug Deliv. Sci. Technol.* **2019**, *53*, 101174. [CrossRef]
3. Nguyen-tri, P.; Nguyen, T.A.; Carriere, P.; Xuan, C.N. Nanocomposite Coatings: Preparation, Characterization, Properties, and Applications. *Int. J. Corros.* **2018**, *2018*, 19. [CrossRef]
4. Tanveer, M.; Farooq, A.; Ata, S.; Bibi, I.; Sultan, M.; Iqbal, M.; Jabeen, S.; Gull, N.; Islam, A.; Khan, R.U.; et al. Aluminum nanoparticles, chitosan, acrylic acid and vinyltrimethoxysilane based hybrid hydrogel as a remarkable water super-absorbent and antimicrobial activity. *Surf. Interfaces* **2021**, *25*, 101285. [CrossRef]
5. Zhang, G.; Li, B.; Liu, J.; Luan, M.; Yue, L.; Jiang, X.T.; Yu, K.; Guan, Y. The bacterial community significantly promotes cast iron corrosion in reclaimed wastewater distribution systems. *Microbiome* **2018**, *6*, 222. [CrossRef]
6. Wang, J.; Liu, G.; Wang, J.; Xu, X.; Shao, Y.; Zhang, Q.; Liu, Y.; Qi, L.; Wang, H. Current status, existent problems, and coping strategy of urban drainage pipeline network in China. *Environ. Sci. Pollut. Res.* **2021**, *28*, 43035–43049. [CrossRef]
7. Sun, H.; Shi, B.; Lytle, D.A.; Bai, Y.; Wang, D. Formation, and release behavior of iron corrosion products under the influence of bacterial communities in a simulated water distribution system. *Environ. Sci. Process. Impacts* **2014**, *16*, 576–585. [CrossRef]
8. Lou, Y.; Chan, W.; Cui, T.; Qian, H.; Huang, L.; Ma, L.; Hao, X.; Zhang, D. Microbiologically influenced corrosion inhibition of carbon steel via biomineralization induced by *Shewanella putrefaciens*. *Mater. Degrad.* **2021**, *5*, 59. [CrossRef]
9. Brindha, T.; Rathinam, R.; Dheenadhayalan, S.; Sivakumar, R. Nanocomposite Coatings in Corrosion Protection Applications: An Overview. *Orient. J. Chem.* **2021**, *37*, 1062–1067.
10. Kausar, A. A review of high performance polymer nanocomposites for packaging applications in electronics and food industries. *J. Plast. Film Sheeting* **2020**, *36*, 94–112. [CrossRef]
11. Zheng, K.; Setyawati, M.I.; Leong, D.T.; Xie, J. Antimicrobial silver nanomaterials. *Coord. Chem. Rev.* **2018**, *357*, 1–17. [CrossRef]
12. Rai, M.; Shegokar, R. Metal Nanoparticles in Pharma. In *Metal Nanoparticles in Pharma*; Springer International Publishing: Cham, Switzerland, 2017; pp. 1–493.
13. Franco, D.; Calabrese, G.; Guglielmino, S.P.P.; Conoci, S. Metal-Based Nanoparticles: Antibacterial Mechanisms and Biomedical Application. *Microorganisms* **2022**, *10*, 1778. [CrossRef]
14. Giraldo Mejía, H.F.; Yohai, L.; Pedetta, A.; Herrera Seitz, K.; Procaccini, R.A.; Pellice, S.A. Epoxy-silica/clay nanocomposite for silver-based antibacterial thin coatings: Synthesis and structural characterization. *J. Colloid Interface Sci.* **2017**, *508*, 332–341. [CrossRef]

15. Hussain, Z.; Tahir, S.A.; Mahmood, K.; Ali, A.; Arshad, M.I.; Ikram, S.; Nabi, M.A.U.; Ashfaq, A.; Rehman, U.U.; Muddassir, Y. Synthesis and characterization of silver nanoparticles with epoxy resin. *Dig. J. Nanomater. Biostructures* **2020**, *15*, 873–883. [CrossRef]
16. Manjumeena, R.; Venkatesan, R.; Duraibabu, D.; Sudha, J.; Rajendran, N.; Kalaichelvan, P.T. Green Nanosilver as Reinforcing Eco-Friendly Additive to Epoxy Coating for Augmented Anticorrosive and Antimicrobial Behavior. *Silicon* **2015**, *8*, 277–298. [CrossRef]
17. Chaudhari, B.; Panda, B.; Šavija, B.; Paul, S.C. Microbiologically Induced Concrete Corrosion: A Concise Review of Assessment Methods, Effects, and Corrosion-Resistant Coating Materials. *Materials* **2022**, *15*, 4279. [CrossRef]
18. Shen, W.; Zhang, T.; Ge, Y.; Feng, L.; Feng, H.; Li, P. Multifunctional AgO/epoxy nanocomposites with enhanced mechanical, anticorrosion and bactericidal properties. *Prog. Org. Coat.* **2021**, *152*, 106130. [CrossRef]
19. Shetty, P.; Bhushan, S.; Vidya, A.; Kodialbail, S. Biocorrosion Behavior of Epoxy—Based Multilayer Nanocomposite Coatings. *J. Bio- Tribo-Corrosion* **2023**, *9*, 45. [CrossRef]
20. Leygraf, C.; Wallinder, I.O.; Tidblad, J.; Graedel, T. Appendix I: The Atmospheric Corrosion Chemistry of Silver. In *Atmospheric Corrosion*, 2nd ed.; John Wiley & Sons, Inc.: Hoboken, NJ, USA, 2016; pp. 337–347.
21. Majeed, H.M.; Wadee, S.A. Antibacterial Activity and Mechanism of Nickel Nanoparticles against Multidrug Resistant *Pseudomonas aeruginosa*. *Ann. Trop. Med. Public Health* **2019**, *22*, 157–168. [CrossRef]
22. *EN 877*; Cast Iron Pipes and Fittings, Their Joints and Accessories for the Evacuation of Water from Buildings—Requirements, Test Methods and Quality Assurance. European Committee for Standardization: Brussels, Belgium, 2006.
23. *ISO/TS 16782*; Clinical Laboratory Testing—Criteria for Acceptable Lots of Dehydrated Mueller-Hinton Agar and Broth for Antimicrobial Susceptibility Testing. International Organization for Standardization: Geneva, Switzerland, 2016.
24. *ISO 22196*; Plastics—Measurement of Antibacterial Activity on Plastics Surfaces. International Organization for Standardization: Geneva, Switzerland, 2007.
25. *ISO 4833–1*; Microbiology of the Food Chain—Horizontal Method for the Enumeration of Microorganisms—Part 1: Colony Count at 30 °C by the Pour Plate Technique. International Organization for Standardization: Geneva, Switzerland, 2018.
26. Ghanbari, A.; Attar, M.M. A study on the anticorrosion performance of epoxy nanocomposite coatings containing epoxy-silane treated nano-silica on mild steel substrate. *J. Ind. Eng. Chem.* **2015**, *23*, 145–153. [CrossRef]
27. Obot, I.B.; Madhankumar, A. Synergistic effect of iodide ion addition on the inhibition of mild steel corrosion in 1 M HCl by 3-amino-2-methylbenzylalcohol. *Mater. Chem. Phys.* **2016**, *177*, 266–275. [CrossRef]
28. Samardžija, M.; Alar, V.; Špada, V.; Stojanović, I. Corrosion Behaviour of an Epoxy Resin Reinforced with Aluminium Nanoparticles. *Coatings* **2022**, *12*, 1500. [CrossRef]
29. Solomon, M.M.; Gerengi, H.; Kaya, T.; Umoren, S.A. Performance Evaluation of a Chitosan/Silver Nanoparticles Composite on St37 Steel Corrosion in a 15% HCl Solution. *ACS Sustain. Chem. Eng.* **2017**, *5*, 809–820. [CrossRef]
30. Anjum, M.J.; Ali, H.; Khan, W.Q.; Zhao, J.; Yasin, G. *Chapter 11—Metal/Metal Oxide Nanoparticles as Corrosion Inhibitors*, 1st ed.; Elsevier: Amsterdam, The Netherlands, 2020; pp. 181–201.
31. Jain, P.; Patidar, B.; Bhawsar, J. Potential ofNanoparticles asa Corrosion Inhibitor: A Review. *J. Bio-Tribo-Corros.* **2020**, *6*, 43. [CrossRef]
32. Geoprincy, G.; Nagendhra Gandhi, N.; Renganathan, S. Novel antibacterial effects of alumina nanoparticles on *Bacillus cereus* and *Bacillus subtilis* in comparison with antibiotics. *Int. J. Pharm. Pharm. Sci.* **2012**, *4*, 544–548.
33. Niroumandrad, S.; Rostami, M.; Ramezanzadeh, B. Effects of combined surface treatments of aluminium nanoparticle on its corrosion resistance before and after inclusion into an epoxy coating. *Prog. Org. Coat.* **2016**, *101*, 486–501. [CrossRef]
34. Samardžija, M.; Kurtela, M.; Vuković Domanovac, M.; Alar, V. Anticorrosion and Antibacterial Properties of Al NP—Epoxy Nanocomposite Coating on Grey Cast Iron. *Coatings* **2023**, *13*, 898. [CrossRef]
35. Feichtenschlager, B.; Pabisch, S.; Svehla, J.; Peterlik, H.; Sajjad, M.; Koch, T.; Kickelbick, G. Epoxy Resin Nanocomposites: The Influence of Interface Modification on the Dispersion Structure—A Small-Angle-X-ray-Scattering Study. Surfaces. *Surfaces* **2020**, *3*, 664–682. [CrossRef]
36. Pavapootanont, G.; Wongpanya, P.; Viyanit, E.; Lothongkum, G. Corrosion behavior of Ni steels in aerated 3.5-wt.% NaCl solution at 25 °C by potentiodynamic method. *Eng. J.* **2018**, *22*, 1–12. [CrossRef]
37. Keast, V.J. Atmospheric Corrosion of Silver and Silver Nanoparticles. *Corros. Mater. Degrad.* **2022**, *3*, 221–234. [CrossRef]
38. Bordbar, S.; Rezaeizadeh, M.; Kavian, A. Improving thermal conductivity and corrosion resistance of polyurea coating on internal tubes of gas heater by nano silver. *Prog. Org. Coat.* **2020**, *146*, 105722. [CrossRef]
39. Asghari, E.; Kaltschmidt, B.P.; van Merwyk, L.; Huser, T.; Kaltschmidt, C.; Hutten, A. *Pseudomonasaeruginosa* Clusters Toxic Nickel Nanoparticles to Enhance Survival. *Microorganisms* **2022**, *10*, 2220. [CrossRef] [PubMed]
40. Hussain, A.; Ahmad, M.N.; Jalal, F.; Yameen, M.; Falak, S.; Noreen, S.; Naz, S.; Nazir, A.; Iftikhar, S.; Soomro, G.A.; et al. Investigating the antibacterial activity of POMA nanocomposites. *Polish J. Environ. Stud.* **2019**, *28*, 4191–4198. [CrossRef]
41. Fonseca, S.; Cayer, M.; Ahmmed, K.M.T.; Khadem-mohtaram, N.; Charette, S.J.; Brouard, D. Characterization of the Antibacterial Activity of an SiO_2 Nanoparticular Coating to Prevent Bacterial Contamination in Blood Products. *Antibiotics* **2022**, *11*, 107. [CrossRef]
42. Mukherjee, A.; Mohammed Sadiq, I.; Prathna, T.C.; Chandrasekaran, N. Antimicrobial activity of aluminium oxide nanoparticles for potential clinical applications. *Sci. Microb. Pathog. Commun. Curr. Res. Technol. Adv.* **2011**, *4*, 245–251.
43. Li, Z.; Ma, J.; Ruan, J.; Zhuang, X. Using Positively Charged Magnetic Nanoparticles to Capture Bacteria at Ultralow Concentration. *Nanoscale Res. Lett.* **2019**, *14*, 195. [CrossRef]

44. Jiang, W.; Mashayekhi, H.; Xing, B. Bacterial toxicity comparison between nano- and micro-scaled oxide particles. *Environ. Pollut.* **2009**, *157*, 1619–1625. [CrossRef] [PubMed]
45. Yasakau, K.A.; Zheludkevich, M.L.; Lamaka, S.V.; Ferreira, M.G.S. Mechanism of corrosion inhibition of AA2024 by rare-earth compounds. *J. Phys. Chem. B* **2006**, *110*, 5515–5528. [CrossRef] [PubMed]
46. Sharmin, S.; Rahaman, M.M.; Sarkar, C.; Atolani, O.; Islam, M.T.; Adeyemi, O.S. Nanoparticles as antimicrobial and antiviral agents: A literature-based perspective study. *Heliyon* **2021**, *7*, 5515–5528. [CrossRef]
47. Gudkov, S.V.; Burmistrov, D.E.; Smirnova, V.V.; Semenova, A.A.; Lisitsyn, A.B. A Mini Review of Antibacterial Properties of Al_2O_3 Nanoparticles. *Nanomaterials* **2022**, *12*, 2635. [CrossRef] [PubMed]